Received: 21 June 2019 | Accepted: 7 February 2020 | Published online: 28 May 2020

DOI: 10.1002/agj2.20180

Agronomy Journal

ARTICLE

Crop Ecology & Physiology

The coordinated increase in stomatal density and vein dimensions during genetic improvement in rice

Lilian Wu[1,2] | **Hugo J. de Boer**[3] | **Zhang Zixiao**[1] | **Xueliang Chen**[1] | **Yanying Shi**[1] | **Shaobing Peng**[1,2,4] | **Fei Wang**[1,2,5]

[1] College of Plant Science and Technology, Huazhong Agricultural University, Wuhan, Hubei 430070, China

[2] MARA Key Laboratory of Crop Ecophysiology and Farming System in the Middle Reaches of the Yangtze River, Wuhan, Hubei 430070, China

[3] Department of Environmental Sciences, Faculty of Geosciences, Utrecht University, Heidelberglaan 2, Utrecht, The Netherlands

[4] National Key Laboratory of Crop Genetic Improvement, Wuhan, Hubei 430070, China

[5] Hubei Collaborative Innovation Center for Grain Industry, Yangtze University, Jingzhou, China

Correspondence
Fei Wang, College of Plant Science and Technology, Huazhong Agricultural University, Wuhan, Hubei 430070, China
Email: fwang@mail.hzau.edu.cn

Abstract

Rice (*Oryza sativa* L. ssp. *indica*) has experienced three distinct phases of considerable yield increases: Green Revolution, utilization of heterosis, and the combination of ideotype and inter-subspecific hybrid breeding. Crop breeding and selection for high yield have increased radiation use efficiency in modern *indica* rice varieties. However, the underlying leaf morphological and physiological changes have not been established. Field and pot experiments were conducted in 2016 and 2017. We investigated the relationships between the anatomical maximum stomatal conductance (g_{max}), operational stomatal conductance (g_{op}), and the anatomy of the stomata and vein in relation to leaf-level transpiration and photosynthesis across historical *indica* rice varieties. The results showed that flag leaf temperature of new varieties was reduced relative to the temperature of older varieties due to increased g_{op} and leaf transpirational cooling. Both high stomatal density and larger veins were increased in new varieties with improved yield potential, while no change was observed in stomatal length and vein density. There was a significant correlation between stomatal density and g_{op} as well as between g_{op} and the light-saturated photosynthetic rate. The present study reveals that historical selection for high yield is accompanied by leaf morphological changes that contribute to enhanced g_{op}, leaf cooling, and photosynthesis of irrigated rice inhabiting hot, high light environments.

1 | INTRODUCTION

Rice (*Oryza sativa L.*) plays a significant role in global food security (Khush, 2001; Ramankutty et al., 2018). Climate warming is expected to negatively affect future rice yield (Challinor et al., 2014; Zhao et al., 2016). Climate warming may be problematic, as climate projections indicate that 27% of the global rice production area will be exposed to at least 5 d of temperatures above the critical temperature threshold during the reproductive period ranging between 34 and 39 °C by 2050 (Gourdji, Sibley, & Lobell, 2013). High temperatures for 1–4 days at the gametogenesis stage could cause a dramatic reduction in spikelet fertility (Endo et al., 2009). A near 2 °C increase in daily temperature decreased the grain yield of *indica* rice by 16.3–21.3% (Shah et al.,

Abbreviations: A, light-saturated photosynthetic rate; g_{max}, the anatomical maximum stomatal conductance; g_{op}, the operational stomatal conductance; iWUE, intrinsic water use efficiency; K_{leaf}, leaf hydraulic conductance; RUE, radiation use efficiency; SLA, specific leaf area; SLN, specific leaf nitrogen content

2014). Despite the potentially adverse effects of ongoing climate change, successful breeding has facilitated significant yield increases over the past century. In general, rice has experienced three distinct phases of considerable yield increases: the Green Revolution, utilization of heterosis, and the combination of ideotype and inter-subspecific hybrid breeding (Cassman, 1999; Yuan, 1997). However, the eco-physiological and anatomical traits of historical rice varieties that contributed to the increase in yield potential remain underexplored.

A clue towards identifying the traits underlying the improvements in rice yield may be found in how radiation use efficiency (RUE) increased over the last 80 years (Zhu et al., 2016). Radiation use efficiency measures the ratio of absorbed radiation relative to the biomass produced, and it fundamentally depends on photosynthetic efficiency and the subsequent conversion of carbohydrates into plant biomass. Interestingly, photosynthetic efficiency has improved little in crops and falls far short of its biological limit (Long, Marshallcolon, & Zhu, 2015), whereas RUE has increased considerably. Shorter, thicker, and erect leaves are selected in rice breeding to increase RUE (Yuan, 1997). The modification of leaf morphology optimizes canopy structure to allow a more uniform light distribution within the canopy (Long et al., 2015). This led to higher light penetration into the canopy (a lower *K*, light extinction coefficient) and more synergetic distribution of light and N within the canopy (Huang, Yang, Li, Peng, & Wang, 2019). A study on soybeans (*Glycine max*; Koester, Nohl, Diers, & Ainsworth, 2016) highlights that daily carbon gain was greater in more recently released varieties, despite observing little improvement in the maximum photosynthetic capacity of this crop. The improvements in daily carbon gain were especially notable in well-watered conditions that enabled high stomatal conductance in soybeans. Indeed, stomatal conductance and productivity are positively correlated across rice genotypes (Roche, 2015).

The apparent close anatomical and physiological coordination of water supply via leaf veins and water loss via stomata plays a crucial role in plant evolution and the ability of plants to adapt to specific environments (Brodribb & Jordan, 2011; Brodribb, Jordan, & Carpenter, 2013; Brodribb, McAdam, & Carins Murphy, 2017; Zhang, Murphy, Cardoso, Jordan, & Brodribb, 2018). As transpiration and CO_2 uptake for photosynthesis are tightly coupled, leaves capable of higher rates of photosynthesis require large numbers of small stomatal pores and a high density of veins (Beerling & Franks, 2010). Crucially, the combination of high stomatal density and small stomatal size is needed to achieve the highest anatomical maximal stomatal conductance (g_{max}; de Boer et al., 2016; Franks & Beerling, 2009). The g_{max} positively correlates with the operational stomatal conductance (g_{op}, a measure of stomatal opening dominated by the stomatal density and apertures of stomata) under typical growth conditions (Farquhar & Sharkey, 1982; Franks, Leitch, Elizabeth, Hetherington, & Beerling, 2012; McElwain, Yiotis, & Lawson, 2016). Moreover, smaller stomata are generally found to exhibit faster opening and closing responses in closely related species of the same genus (Drake, Froend, & Franks, 2013; Hetherington & Woodward, 2003; Lawson & Vialet-Chabrand, 2019). McAusland et al. (2016) further demonstrated that smaller stomata facilitate the synchronization of stomatal and photosynthetic responses to light.

Core Ideas

- Genetic improvement in rice yield increased stomatal density and vein area.
- New varieties had higher stomatal conductance and lower leaf temperature.
- Photosynthetic rate is significantly correlated with stomatal conductance.

Improvements in leaf water transport and transpiration may improve photosynthetic efficiency through enhancing transpirational cooling. The thermal response curve of light-saturated photosynthetic rate (*A*) usually peaks between 25 and 30 °C in C_3 photosynthetic species (Xiong, Ling, Huang, & Peng, 2017; Yamori, Hikosaka, & Way, 2014). Leaf temperature is determined by the energy balance between the leaf interior and the ambient environment (Campbell & Norman, 1998) and may be regulated by leaf physical traits and transpiration (Defraeye, Verboven, Ho, & Nicolai, 2013). In cotton (*Gossypium* L.) and wheat (*Triticum aestivum*), yields are positively correlated with g_{max} but not with photosynthesis (Lu, Percy, Qualset, & Zeiger, 1998). This is because high stomatal conductance leads to significant transpirational cooling of irrigated crops to temperatures below the threshold for yield reduction (Hetherington & Woodward, 2003).

We hypothesized that the observed improvements in RUE in rice are related to the adjustments in leaf morphology and anatomy affecting stomatal conductance and transpirational cooling. We explored our hypothesis by determining the anatomy of stomata and veins for the historical rice varieties and evaluated the effects of the anatomical variations on the operational stomatal conductance, leaf temperature, and photosynthetic capacity. The Yangtze River Valley is one of the most important rice-producing regions in China but is prone to rice yield loss due to high temperatures (Shah et al., 2014). For our experiments, we selected 20 historical *indica* rice varieties from the Yangtze River Valley. The 20 varieties were grown in field trials in

2016 and 2017. A subset of eight varieties were grown in a pot experiment in 2017. We also grew eighteen *japonica* rice (*Oryza sativa* L. ssp. *japonica*) varieties that were planted in a temperate climate. This combination of field and pot experiments allows us to explore the eco-physiological and anatomical traits that contributed to the increase in RUE and grain yield in historical *indica* rice varieties.

2 | MATERIALS AND METHODS

2.1 | Plant material and growth conditions

The field trials and experiments were conducted at the experimental farm of Huazhong Agricultural University (114°37′E, 30°48′N), Wuhan, Hubei, China, during the rice-growing season from May to October in 2016 and 2017. Soil from the experimental field had a texture of clay loam with pH 6.17, organic matter 11.23 g kg^{-1}, total N 0.9 g kg^{-1}, available P 10.42 mg kg^{-1}, and available K 133.85 mg kg^{-1}.

Twenty historical *indica* rice varieties released from 1936 to 2015 were grown in 2016 and 2017. The varieties were selected to represent four distinct historical groups (see Supplemental Table S1), representing the historical developments in crop breeding. Varieties from the 1930s–1950s (growth duration of 106–117 d) were all inbred varieties with tall stature, while varieties from the 1960s–1970s (growth duration of 117–146 d) were all inbred varieties with semi-dwarf stature. The other two groups, namely, the 1980s–1990s (growth duration of 117–133 d) and 2000s (growth duration of 129–133 d), included both inbred and hybrid varieties. In 1996, the Ministry of Agriculture (MOA) in China launched a national project to breed Super Hybrid Rice through the combination of intersubspecific heterosis and ideotype (Yuan, 1997). The LYPJ, YLY900, YLY6, and SLY5814 varieties from the 2000s were all super hybrid rice varieties designated by the MOA. The HHZ (Huang-Hua-Zhan) variety was the inbred rice variety with the largest planting area in the last decade in South China. Overall, the 20 varieties were all cultivated as middle-season rice in a large-scale area during their respective period in the Middle Reaches of the Yangtze River of China (Supplemental Table S1).

In 2016, 12 historical *japonica* rice varieties released from the 1950s to the 2000s were also used in the field experiment. Those varieties were all inbred varieties separated into six groups based on their release decade (Supplemental Table S1).

All rice varieties were arranged in a complete randomized design with three replications. The plot size was 3 by 4 m in 2016 and 4 by 5 m in 2017. Pre-germinated seeds were sown in the seedbeds. Seedlings (25 d old) were transplanted on 11 June 2016, and 27-d-old seedlings were transplanted on 6 June 2017. The planting density was 25 hills m^{-2} at a hill spacing of 20.0 by 20.0 cm with two seedlings per hill.

Fertilizers including urea for N, single superphosphate for P, and potassium chloride for K were applied at rates of 100 kg N ha^{-1}, 40 kg P ha^{-1}, and 100 kg K ha^{-1}. N fertilizers were applied at splits of 4:3:3 at basal (1 d before transplanting), tillering (7 d after transplanting), and panicle initiation. All P fertilizers were applied as basal fertilizer. K fertilizer was applied at splits of 1:1 at basal (1 d before transplanting) and panicle initiation. The experimental field was flooded from transplanting until 7 d before maturity. Pests and weeds were intensively controlled using chemicals to avoid yield loss.

An additional pot experiment was conducted to investigate the gas exchange of *indica* rice varieties released in different decades. Eight varieties were chosen from the 20 rice varieties to carry out the pot experiment, with two varieties from each group. After germination on moist filter paper on 9 May 2017, the seeds were transferred to nursery plates (55 cm^3 for each hole) filled with soil. When the seedlings had developed an average of 2.5 leaves, they were transplanted into 10.0-L pots (23-cm diameter; 27-cm height) with a density of three hills per pot and two seedlings per hill (six seedlings per pot and four pots for each variety). Each pot was filled with 10.0 kg of soil; compound fertilizer was applied as basal fertilizers with 1.56 g (0.23 g N, 0.23 g K_2O, and 0.23 g P_2O_5) per pot by incorporation into the soil. After transplanting, the rice plants were placed outdoors. During the entire growth season, rice plants were well watered, and a minimum 2-cm water layer was maintained to avoid drought stress.

2.2 | Operational stomatal conductance and leaf temperature

The g_{op} was measured on the *indica* rice varieties in the field trials from 8:00 a.m. to 2:00 p.m. during the heading stage as well as 64 and 70 d after sowing (DAS64 and DAS70, respectively) using a leaf porometer (SC-1, Decagon, Pullman, WA). Three topmost fully expanded leaves were selected for the measurement in each plot. Additional measurements of leaf and air temperature were performed at DAS64 and DAS69 at 12:00 p.m. and at DAS70 from 8:00 a.m. to 2:00 p.m. in 2017 using a thermocouple device (AZ Instrument, TaiChung, Taiwan) by attaching one thermo sensor to the middle part of the newest fully expanded leaves. The air temperature was recorded at the same time by putting the other thermo sensor in the air (Huang, Zhang, Wei, Peng, & Li, 2017; Koike et al., 2015).

2.3 | Measurement of leaf gas exchange

Plants grown outdoors in pot experiment were transferred into an environmental controlled room (air temperature of 27.8 ± 2.1 °C, the photosynthetic photon flux density (PPFD) at leaf surface of 1200 ± 47 μmol m^{-2} s^{-1}, and relative humidity of 77.4 ± 5.3%) at booting stage (about 7 d before heading). Plants were adapted to the environment for 1 d before gas exchange measurement. Gas exchange measurements were performed between 09:00 a.m. and 3:30 p.m. using an LI-6400XT portable photosynthesis system (Li-Cor, Lincoln, NE), One flag leaf per hill (three hills per pot and four pots for each variety) was selected to measure the light-saturated photosynthetic rate (A) and stomatal conductance (g_{op}). The PPFD during these measurements was set at 1,500 μmol photons m^{-2} s^{-1} using a red-blue light-emitting diode artificial light source. The leaf-air vapor pressure deficit (vpd) was controlled at approximately 2.0 kpa, and the CO_2 concentration in the leaf chamber was adjusted to 400 μmol mol^{-1} with a CO_2 mixture.

2.4 | Leaf morphological and functional traits

From the field trials, the seventh and flag leaves were sampled in 2016, and only the flag leaf was sampled in 2017. For each plot, the representative topmost fully expanded leaf was sampled from nine hills. Leaves used for measuring gas exchange in the pot experiment were harvested to determine their morphological traits on the consecutive day. The leaf area was measured with a Li-Cor area meter (Li-Cor Model 3100, Li-Cor, Lincoln, NE). Leaves were subsequently oven-dried at 80 °C to achieve a constant weight and were ground with a mixer mill homogenizer (MM400, Retsch, Haan, Germany). Thereafter, approximately 3.8 mg of dry leaf material was used to measure N concentration using an NC analyzer (IsoPrime100 IRMS, Elementar, Langenselbold, Germany). Specific leaf area (SLA) was calculated from the leaf area and dry weight:

$$\mathrm{SLA} = \frac{\text{leaf area}}{\text{leaf dry weight}} \tag{1}$$

2.5 | Stomatal morphology

Leaves sampled from the field trials similar to that used for leaf morphological traits were used for stomatal analyses. The improved scratching method was used to determine leaf stomatal density which was expressed as the number of stomata per unit leaf area (Radoglou & Jarvis, 1990). The leaf samples were fixed in formalin acetic acid-alcohol (FAA) solution (500 ml absolute ethanol, 270 ml formaldehyde, 50 ml acetic acid, 180 ml water). The adaxial surface of the leaf was removed by gentle scratching, and the stomatal density of the abaxial surface was observed using a light microscope (Nikon, ECLIPSE Ti, Tokyo, Japan). The number of stomata were counted under 200-fold magnification (10 × 20), and guard cell length was determined by measuring guard cell length under (10 × 40) 400-fold magnification. Guard cell length was measured between the junctions of the guard cells at each end of the stomata. Both traits were measured with ImageJ software (the National Institutes of Health, Bethesda, MD; https://imagej.nih.gov/ij/).

Theoretical maximum stomatal conductance (g_{max}) was calculated using the guard cell length and stomatal density of the closed stomata following the equation (Franks et al., 2014):

$$g_{\max} = \frac{d}{v} D a_{\max} \Big/ \left(l + \frac{\pi}{2} \sqrt{\frac{a_{\max}}{\pi}} \right) \tag{2}$$

where d is the diffusivity of CO_2 in air at 25 °C (0.0000249 m^2 s^{-1}), v is the molar volume of air (0.0224 m^3 mol^{-1}), and D is stomatal density, $a_{\max} = \beta(\pi p^2/4)$, which is defined as a fraction β accounting for the shape of the stomatal pore at maximum aperture. A value of $\beta = 1.0$ represents a circular pore with pore length equal to diameter, while the long narrow stomata of our rice varieties are best represented with the factor $\beta = .4$ (Franks et al., 2014). In the field experiment of 2017, guard cell width of l and stomatal pore length (p) of 25 closed stomata were measured from the 400-fold magnified images to calculate g_{max} (Supplemental Figure S1). Guard cell width was measured here instead of depth because the depth of the stomatal pore is hard to measure and approximately equals to the width of the inflated guard cell (refer to Supplemental Figure S2 in the supplementary text_01 of Franks et al., 2014).

2.6 | Leaf vascular traits

Rice veins appear as white parallel bands on a green background on the leaf surface. Veins were imaged using a bright field microscope (Nikon, ECLIPSE Ti, Tokyo, Japan). Vein number per mm was counted using ImageJ software (the National Institutes of Health, Bethesda, MD; https://imagej.nih.gov/ij/).

To determine the traits of bundle sheath cells, samples of flag leaves were fixed in FAA for at least 12 h. The samples were cross sectioned by hand using a razor blade.

Leaf sections were placed in 85% (v/v) ethanol for 24 h, after which the ethanol was removed and rinsed off with water. A fresh application of 85% (v/v) ethanol was then applied for 24 h. The ethanol was removed and rinsed off with water after this period and replaced by 1% aniline blue in 2016. In 2017, the leaf sections were stained using safranin-fast green. Photos from these samples were taken at 200× magnification using a light microscope (Nikon, ECLIPSE Ti, Tokyo, Japan).

At 200× magnification, the bundle sheath cells could be viewed. Measurements of leaf large vein height and width, small vein height and width, and the number of bundle sheath cells were performed for flag leaves (Supplemental Figure S1). The average width and height of the small vein were 47.5 and 46.9 μm, respectively for the 20 varieties, and they were 120.8 and 133.7 μm, respectively for the large veins. Therefore, the vein area of the large vein and small vein was calculated following Equation 2, assuming that the veins have a circular cross section.

$$\text{Vein area} = \frac{\pi(\text{vein height})(\text{vein width})}{4} \quad (3)$$

2.7 | Measurement of carbon isotope discrimination

The leaves for morphological and functional traits were dried in an oven at 80 °C and 1.1- to 1.3-mg leaf samples were used for analysis by Isoprime100 (Elementar, Langenselbold, Germany). The ratio of ^{13}C to ^{12}C (δ) is reported relative to the Pee Dee Belemnite standard. Based on the equation from Farquhar, Ehleringer, and Hubick (1989), the carbon isotope composition (δ_p) was calculated as:

$$\delta_p = \frac{R_P - R_S}{R_S} = \frac{R_P}{R_S} - 1 \quad (4)$$

where R_S is the molar abundance ratio ($^{13}C/^{12}C$) of the PDB standard (carbon isotopic ratio in CO_2 generated from a fossil belemnite from the Pee Dee Formation), and R_P is the molar abundance ratio ($^{13}C/^{12}C$) of a plant sample. Carbon isotope discrimination (Δ, ‰) was calculated as:

$$\Delta = \frac{R_a}{R_p} - 1 = \frac{\delta_a - \delta_p}{1 + \delta_p} \quad (5)$$

where R_a is molar abundance ratio ($^{13}C/^{12}C$) in air, and δ_a is the ratio of $^{12}C/^{13}C$ of free atmospheric CO_2 on the PDB scale and is approximately −8‰ according to the Earth System Research Laboratory (National Oceanic and Atmospheric Administration, U.S. Department of Commerce, 325 Broadway Boulder, Colorado).

2.8 | Statistical analysis

One-way analysis of variance (ANOVA) was used to test the differences in measured traits using Statistix 8.0. Means of the four groups of release decades were compared based on the least significant difference (LSD) test at the .05 probability level. Graphs were created using Sigmaplot 12.5 (Systat Software, San Jose, CA). The correlations were analyzed using SigmaPlot 12.5, and the regressions that are best fit for the data are shown in the figures.

3 | RESULTS

3.1 | Growth duration

The heading date and total growth duration of the *indica* rice varieties were recorded in 2016. The heading time was 78 ± 3.9 d for the varieties released in the 1930s–1950s, 88 ± 12.6 for that in the 1960s–1970s, 90 ± 2.2 for that in 1980s–1990s, and 91 ± 2.5 for that in 2000s. Accordingly, the total growth duration was 111 ± 5.5 d, 126 ± 13.2, 127 ± 6.1, and 132 ± 1.8 for the four variety groups, respectively. For *japonica* rice varieties, the heading time was 89–92 d except for varieties released in 1970s (81 d), whereas the total growth duration was 146–147 d except for varieties released in 1950s (125 d) and 1970s (131 d).

3.2 | Leaf morphology

Genetic improvement in *indica* rice has changed leaf morphology. Newer varieties tended to have shorter, thicker leaves than older varieties, as shown by their smaller SLA and higher specific leaf N content (SLN; Figure 1). No difference was observed in leaf width (Supplemental Table S2).

3.3 | The operational stomatal conductance and leaf temperature

In order to identify traits that have changed as a result of breeding for high yield in rice, g_{op} and the difference between leaf temperature and air temperature ($\Delta T_{l\text{-}a}$) were measured at different growth stages (Figure 2). The g_{op} increased with the release decades (Figure 2a), whereas $\Delta T_{l\text{-}a}$ decreased during the period of genetic improvement

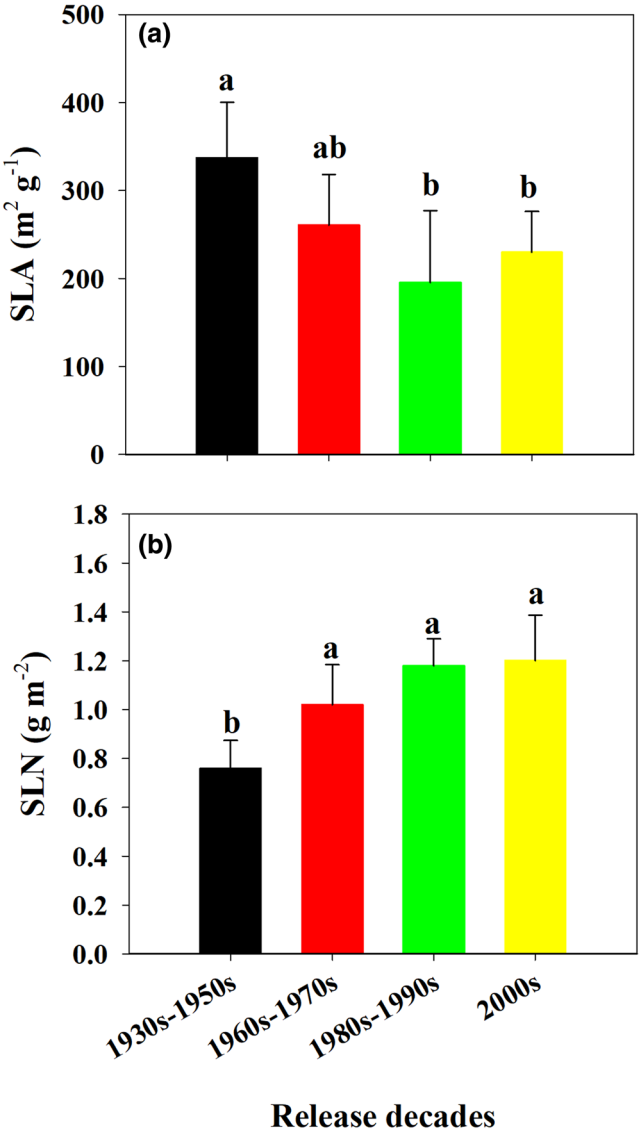

FIGURE 1 The specific leaf area (SLA; a) and specific leaf nitrogen (SLN; b) of flag leaf for *indica* rice varieties released in different decades in 2017. Letters indicate significant differences among group means (LSD $p < .05$). The error bars represent standard deviations. Data was obtained from the 20 varieties cultivated in the field

(Figure 2b). A negative correlation was observed between g_{op} and $\Delta T_{l\text{-}a}$ measured on the same day ($r = .76$, $p < .001$, Figure 2c). The average carbon isotope discrimination ($\Delta^{13}C$) among varieties released in different decades was similar; however, the new varieties showed smaller genotypic variation than the old varieties (Figure 3).

3.4 | Theoretical maximum stomatal conductance and vein density

To explain the trend in g_{op} among varieties released in different decades, the theoretical maximum stomatal conductance (g_{max}) also increased with breeding progress (Figure 4a). There was a quadratic relationship between the g_{op} of the flag leaf at the heading stage and the corresponding g_{max} ($r^2 = .46$, $p < .01$, Figure 4b). This suggests that increases in g_{op} saturate at higher levels of g_{max}, and g_{op} is not necessarily constrained by g_{max} in varieties with high stomatal density, but possibly by stomatal opening. The ratio of g_{op}/g_{max} remained relatively stable at approximately 0.4 for different variety groups (Figure 4c). Vein density was measured as it affects the stomatal conductance (Boyce, Brodribb, Field, & Zwieniecki, 2009) and photosynthetic rate (Brodribb & Jordan, 2007), whereas no differences in vein density were found among variety groups from different decades (Figure 4d).

3.5 | Covariation of stomata and leaf venation traits

Increases in stomatal density of the flag leaf were observed among the *indica* varieties along with the breeding progress (Figure. 5a). Similar results were found in the seventh leaf (Supplemental Figure S2a). No significant difference in stomatal length was observed among different variety groups in 2016 and 2017 (Figure 5b). The leaf vein area of both the large and small veins increased along with the release decades in both 2016 and 2017 (Figure 5c and 5d). A significant correlation was observed between stomatal density and vein area, especially for small veins ($r = .62$, $p < .01$ in 2016; $r = .50$, $p < .05$ in 2017; Figure 6).

3.6 | Physiological traits related to photosynthesis

We further tested whether the physiological traits related to photosynthesis also changed in a similar way with leaf anatomy as breeding progressed. Two varieties in each group were selected randomly for the determination of A, stomatal conductance (g_{op}), SLN, and intrinsic water use efficiency (iWUE, defined as A/g_{op}) at the heading stage in 2017 (Table 1). The variation in stomatal density, SLA, and SLN along with the breeding process in the pot experiment was similar to that found in the field experiments (Table 1; Figures 1 and 5a). There were differences in A, g_{op}, and iWUE among the eight varieties (Table 1). The variation in g_{op} was correlated with the change in stomatal density in a quadratic manner ($r = .82$, $p < .05$; Figure 7a). A significantly and linearly correlated with g_{op} ($r = .89$, $p < .01$; Figure 7b) but not SLN ($r = .35$; Figure 7c).

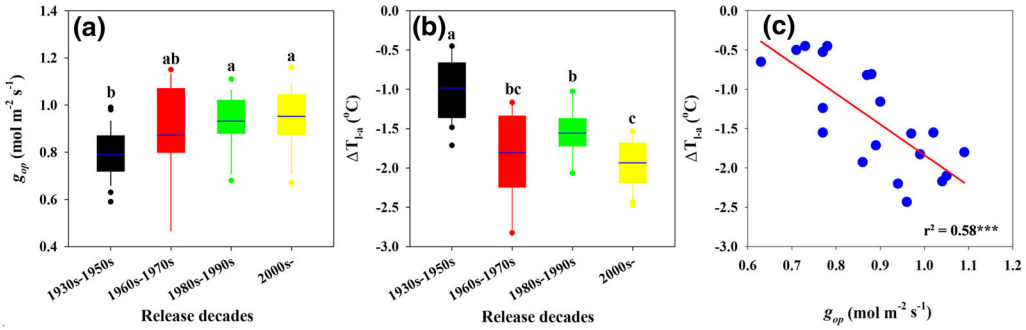

FIGURE 2 The operational stomatal conductance (g_{op}; a) and the difference between leaf and air temperature ($\Delta T_{l\text{-}a}$; b) of the *indica* rice varieties released in different decades measured between 8:00 a.m. and 2:00 p.m. at different growth stages in 2017, and the relationship between g_{op} and $\Delta T_{l\text{-}a}$ measured simultaneously between 8:00 a.m. and 2:00 p.m. at 70 d after sowing (c). Different letters indicate significant differences among group means (LSD $p < .05$). The outer box edges represent the 25th and 75th percentiles, the error bars are the 5th and 95th percentiles, and the blue lines represent the mean values. r^2 is the regression coefficient. *** represents significance at $p < .001$. $\Delta T_{l\text{-}a} = T_{leaf} - T_{air}$. Data was obtained from the 20 varieties cultivated in the field

TABLE 1 Stomatal density, specific leaf area (SLA), specific leaf nitrogen (SLN), light saturated photosynthetic rate (A), stomatal conductance (g_s), and intrinsic water use efficiency (iWUE) of the flag leaves in pot experiment 2017

Release decades	Variety	Stomatal density	SLA	SLN	A	g_s	iWUE
		mm^{-2}	$g\ cm^{-2}$	$g\ m^{-2}$	$\mu mol\ m^{-2}\ s^{-1}$	$mol\ m^{-2}\ s^{-1}$	$\mu mol\ mol^{-1}$
1930s–1950s	WLX	452d[a]	218.0c	1.12bcd	16.1c	0.23c	72.9a
	SLX	495bcd	302.9a	0.90d	20.0a	0.36b	55.6b
1960s–1970s	EZ2	564abc	297.0ab	1.08bcd	21.4a	0.48a	45.4cd
	NJ11	490cd	266.2b	0.99cd	16.7bc	0.31b	54.5b
1980s–1990s	SY63	618a	193.9c	1.41a	20.5a	0.54a	39.0d
	YD6	631a	225.5c	1.17abc	21.5a	0.48a	45.2cd
2000s	YLY6	575ab	205.7c	1.31ab	21.7a	0.52a	41.4d
	HHZ	610a	224.1c	1.27ab	19.2ab	0.37b	51.8bc

[a]Within a column in a leaf, means followed by different letters are significantly different from each other based on LSD (.05). $n = 9$, 11, 6, 6, 3, 4, 3, and 6 for WLX, SLX, EZ2, NJ11, SY63, YD6, YLY6 and HHZ, respectively, for the measurement of A and g_s. T_{leaf} was around 35 °C.

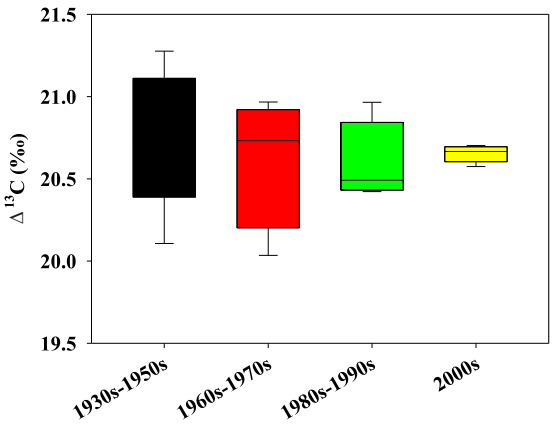

FIGURE 3 The ^{13}C discrimination of the flag leaf in the varieties released at different decades in the field experiment of 2016. The outer box edges represent the 25th and 75th percentiles, the error bars are the 5th and 95th percentiles, and the blue lines represent the mean values. Data was obtained from the 20 varieties cultivated in the field

4 | DISCUSSION

4.1 | Coordination of the stomata and vein during genetic improvement in rice

The optimization of gas exchange in environments that suffer water deficits may select for species with high densities of small stomata (de Boer, Eppinga, Wassen, & Dekker, 2012; Franks & Beerling, 2010); however, the requirement for leaf cooling in hot climates with high light intensities may select for species with moderate densities of midsized stomata (McElwain et al., 2016). A significant negative correlation has been widely observed in different species between stomatal density and size, both of which determine the g_{max} (de Boer et al., 2016; Franks & Beerling, 2009). In present study, the stomatal density of *indica* rice varieties increased with the 80-yr

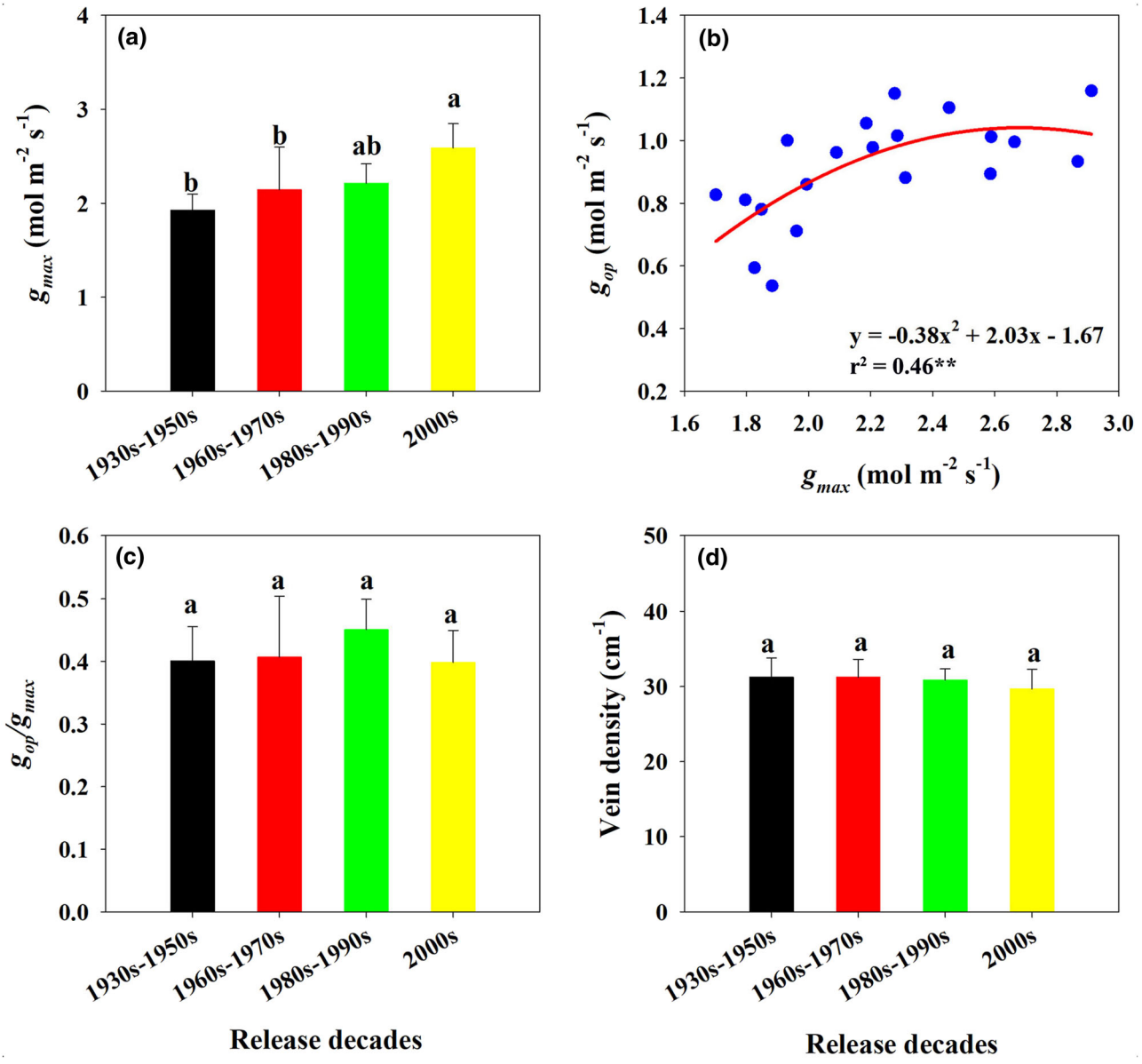

FIGURE 4 The theoretical maximum stomatal conductance (g_{max}; a), the relationship between operational stomatal conductance (g_{op}) and g_{max} (b), the ratio of g_{op} and g_{max} (g_{op}/g_{max}; c), and vein density (d) for *indica* rice varieties released in different decades in 2017. In a, c, and d, the error bars represent standard deviations. In panel a, c, and d, different letters indicate significant differences among group means (LSD $p < .05$). r^2 is the regression coefficient, and ** represents significance at $p < .01$. Data was obtained from the twenty varieties cultivated in the field

high-yield breeding process (Figure 5a). However, no significant change was observed in stomatal length along with the breeding process (Figure 5b).

Stomatal density and length showed no clear trend during the breeding process of *japonica* rice varieties (Supplemental Table S2), which are more adapted to temperate environments (Liu et al., 2018; Ma et al., 2015). It is noteworthy that the old *indica* and *japonica* varieties have comparable stomatal density; however, the stomatal density of the new *indica* varieties is substantially higher than that of the corresponding *japonica* varieties. Hence, our study supports the hypothesis that a high density of stomata confers better adaptation of irrigated *indica* rice to a habitat with high temperature and radiation (McElwain et al., 2016).

The design and function of leaf venation are important for plant adaptation across environments (Sack & Scoffani, 2013). The diameters of whole veins can reflect differences in transport capacity when they contain greater sizes and numbers of xylem and phloem cells (Coomes, Heathcote,

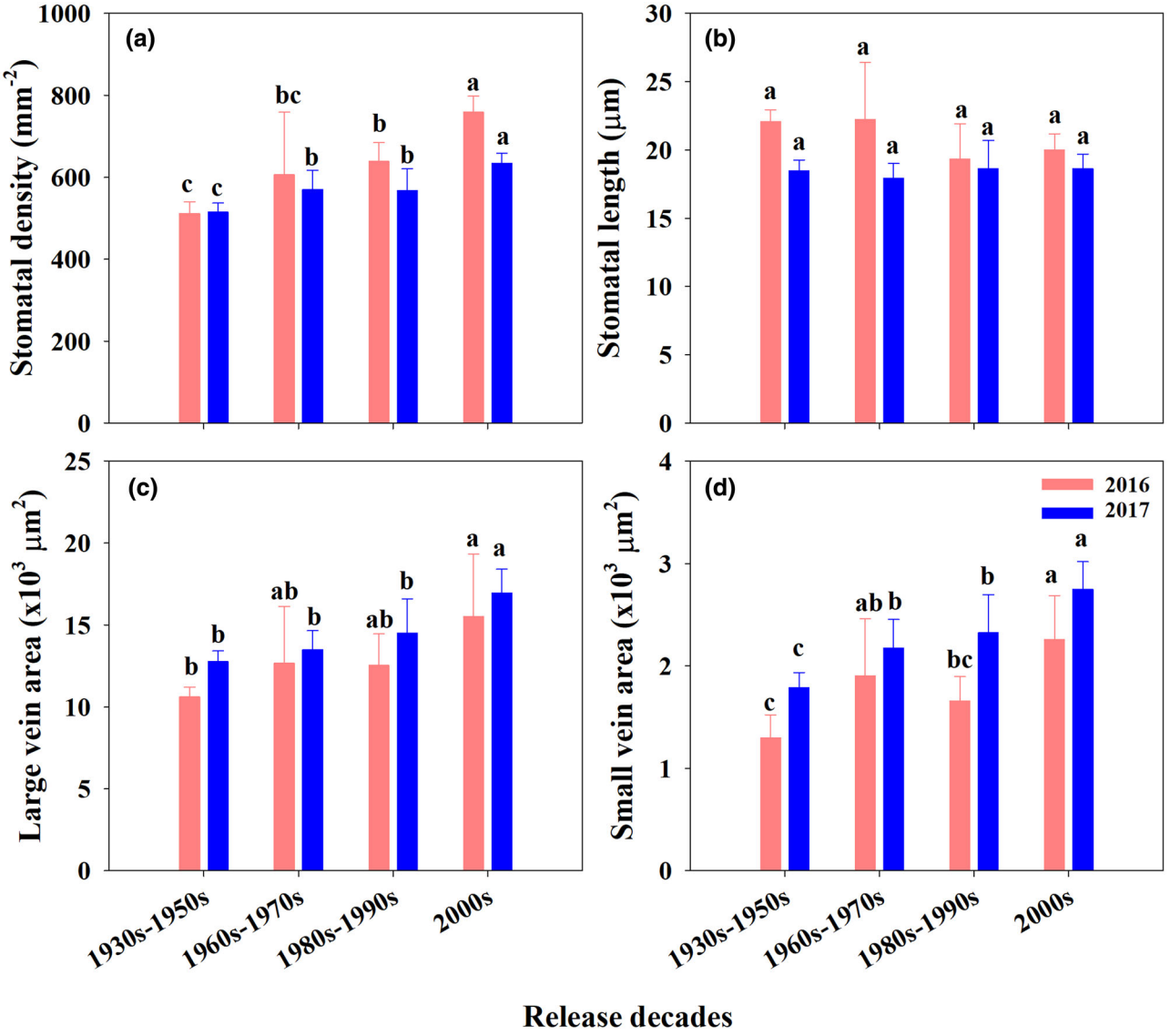

FIGURE 5 Stomatal density (a), stomatal length (b), large vein area (c), and small vein area (d) of flag leaf for *indica* rice varieties released in different decades in 2016 and 2017. The error bars represent standard deviations. Different letters indicate significant differences among group means in each year (LSD $p < .05$). Data was obtained from the 20 varieties cultivated in the field

Godfrey, Shepherd, & Sack, 2008; Taneda & Terashima, 2012). In the present study, significant enlargement in the vein dimensions of both large and small veins was observed along with the release decades (Figure 5c and 5d), but there was no change in vein density (Figure 4d). Stomatal density significantly correlated with the size of both large and small veins (Figure 6; Supplemental Figure S3). The coordination of vein and stomatal densities in various species has been found in evolution and across environments, reflecting an optimization of the trade-off between transpirational costs to plants and CO_2 assimilation (Brodribb et al., 2017). However, separate mechanisms defining vein and stomata development were also found in *Pisum sativum* (McAdam et al., 2017) and *Rheum rhabarbarum* (Cardoso, Randall, Jordan, & McAdam, 2018).

4.2 | Potential effects of g_{op} on transpirational cooling and RUE

Genetic improvement in yield potential was accompanied by an increase in RUE in soybean and rice (Koester, Skoneczka, Cary, Diers, & Ainsworth, 2014; Zhu et al., 2016), which was possibly ascribed to high g_{op} in new

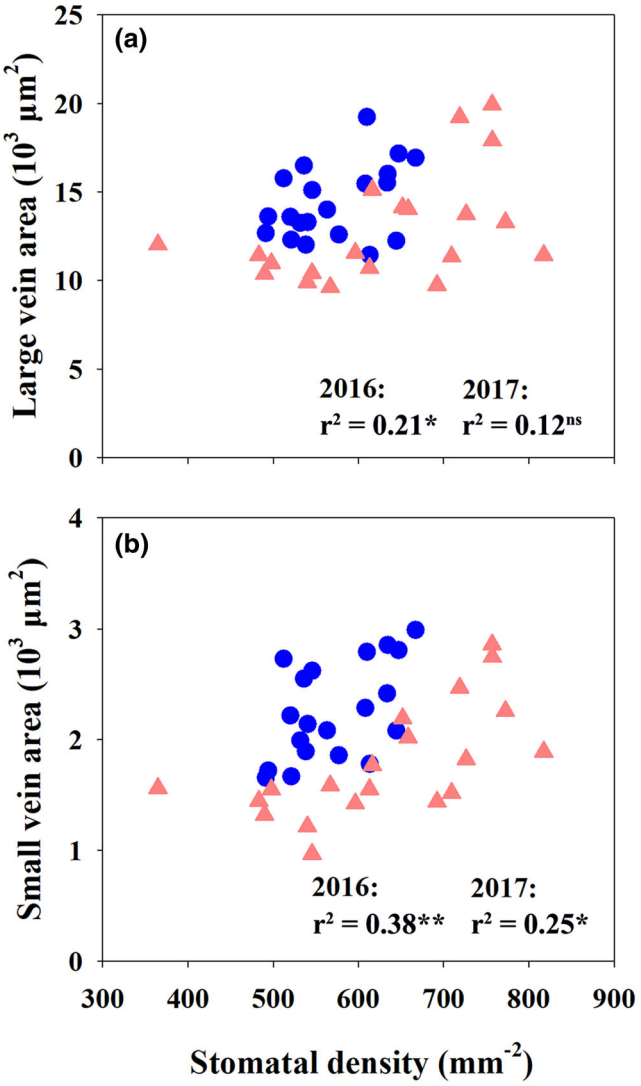

FIGURE 6 The relationship between stomatal density and vein area of the large vein (a) and small vein (b) of the flag leaf for *indica* rice varieties released in different decades in 2016 (pink triangles) and 2017 (blue circles). r^2 is the regression coefficient. *, **, and ns represent significance at $p < .05$, $p < .01$, and nonsignificant, respectively. Data was obtained from the 20 varieties cultivated in the field

varieties (Roche, 2015). Here, it was found that g_{op} measured in the field conditions was significantly increased in more recently released *indica* varieties than that in older varieties. A positive correlation between g_{max} and g_{op} was observed, whereas a negative correlation between g_{op} and $\Delta T_{l\text{-}a}$ was observed (Figures 2c and 4b). These associations highlight the selection for varieties with traits that contribute to high transpirational cooling under non-limited water conditions. Tholen, Boom, and Zhu (2012) summarized that erect leaves can become too hot under direct sunlight without high transpiration rates. High temperature could inhibit Rubisco activity (Crafts-Brandner & Salvucci, 2000), increase photorespiration (Gandin, Koteyeva, Voznesenskaya, Edwards, & Cousins, 2014), decrease the electron transport rate (Sage & Kubien, 2007), accelerate photoinhibition under high light conditions (Takahashi & Murata, 2008), and slow the response of A and g_{op} to dynamic light (Huang et al., 2017) Therefore, leaf transpirational cooling in more recently released *indica* rice varieties possibly alleviated the adverse effects of high temperature on CO_2 assimilation and facilitate the increase in daily carbon accumulation as found in soybean (Koester et al., 2016).

The mathematical model from Farquhar et al. (1989) predicts a strong relationship between $\Delta^{13}C$ and water use efficiency. In C_3 plants, differences in carbon isotope composition are principally associated with discrimination by Rubisco and diffusion of CO_2 from the atmosphere to the chloroplast (Farquhar et al., 1989). Here, the comparable values in $\Delta^{13}C$ for varieties released in different decades indicated that the increase in transpiration was accompanied by an increase in carbon accumulation. This was consistent with the trend of iWUE in the pot experiment (Table 1).

4.3 | Effects of the higher stomatal density and enlarged vein dimensions on CO_2 assimilation

In the present study, significant correlations between stomatal density and g_{op}, as well as between g_{op} and A were observed among the eight varieties released in different decades (Figure 7). The correlation between A and g_{op} has been widely acknowledged for some time (Wong, Cowan, & Farquhar, 1979). By investigating the most productive rice variety in Japan (an *indica* variety Takanari), it was found that the high A of Takanari was related to its high g_{op} (Taylaran, Adachi, Ookawa, Usuda, & Hirasawa, 2011). Elevated g_{op} in a rice mutant deficient in SLAC1 (a guard cell anion channel protein) also results in increased photosynthesis (Kusumi, Hirotsuka, Kumamaru, & Iba, 2012). In *Arabidopsis*, the increase in stomatal density by overexpressing *STOMAGEN* results in a significant increase in g_{op} and a 30% increase in A compared to wild-type plants (Tanaka, Sugano, Shimada, & Hara-Nishimura, 2013). High g_{op} could also speed the response of A to fluctuating light in *Arabidopsis* (Kaiser et al., 2016).

The concomitant increase in vein size may contribute to the increase in g_s possibly through the effects of veins on leaf hydraulic conductance (K_{leaf}; Figures 5 and 6; Brodribb & Jordan, 2007). The relationship between K_{leaf} and g_{op} as well as between K_{leaf} and A has been observed in different species, including rice (Brodribb

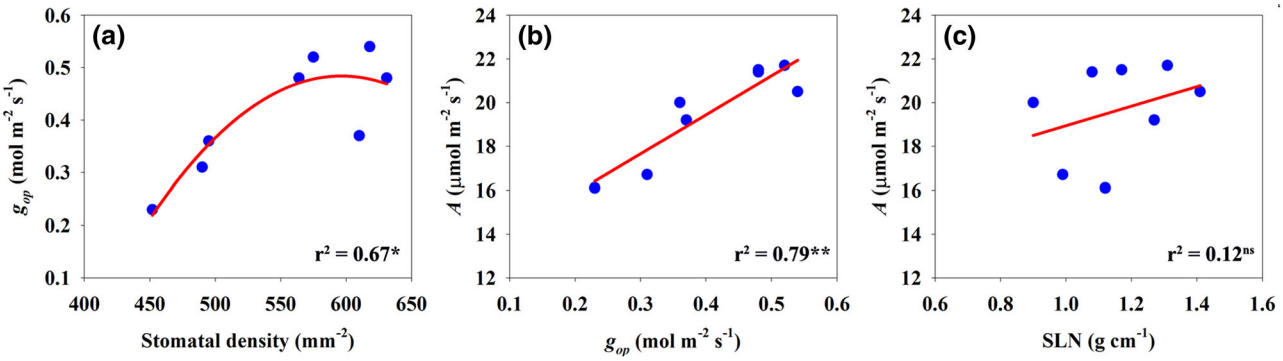

FIGURE 7 The relationship between stomatal density and g_{op}, g_{op}, and A, specific leaf N content (SLN) and A in flag leaf at heading stage for *indica* rice varieties released in different decades in pot experiment of 2017. r^2 is the regression coefficient. *, **, and ns represent significance at $p < .05$, $p < .01$, and nonsignificant, respectively. Data was obtained from the eight varieties cultivated in the pots

& Jordan, 2007; Hubbard, Ryan, Stiller, & Sperry, 2001; Xiong et al., 2015). In addition to the effect of vein density on K_{leaf}, g_{op} and A, other vein traits, such as xylem conduit numbers and diameters, free-ending veins, bundle sheath anatomical traits, and the total area of mesophyll cells per leaf area, also influence K_{leaf} (Caringella, Bongers, & Sack, 2015).

Here, we also observed a significant increase in SLN and a decrease in SLA along with the breeding process, which together with the change in leaf anatomy led to higher A (Table 1). Recent evidence points towards coordinated developmental processes in the epidermis and mesophyll tissues of leaves: anatomical g_{max} has been correlated with leaf N content and the maximum rate of Rubisco carboxylation (V_{cmax}) in evolution, across environments, and during artificial breeding (Franks & Beerling, 2010; Koester et al., 2016). In rice, K_{leaf} is significantly correlated with leaf matter per area and SLA across four rice cultivated cultivars and seven wild cultivars in the genus *Oryza* (Xiong et al., 2015). Moreover, for the most productive rice variety in Japan, high SLN also contributes to the high A in addition to g_{op} (Taylaran et al., 2011). In present study, both SLN and g_{op} contributed to the increase in A for the new released varieties, but g_{op} made a larger contribution than SLN (Figure 7b and 7c). This was possibly due to the larger range in g_{op} variation compared with SLN among the eight varieties.

5 | CONCLUSIONS

Our study shows how coordinately optimized stomata and vein structures potentially facilitate the achievement of high RUE in rice under a continuously warming climate by increasing leaf transpirational cooling and the photosynthetic rate. Our study also demonstrates the frequently observed covariation between stomata and vein traits across species in the artificial breeding process of one species. Genetic mechanisms controlling this coordinated development of stomata and vein, epidermal and mesophyll cells warrant systematic investigation.

ACKNOWLEDGEMENTS

This work was supported by the Program of National Natural Science Foundation of China (No. 31501255), the National Key Research and Development Program of China (No. 2017YFD0301401-3), and an NWO Veni grant supporting H.J.B.

AUTHOR CONTRIBUTIONS

L.W. was responsible for the experimental work and took joint responsibility with F.W. for writing the manuscript and drawing the figures. Z.Z., X.C., and Y.S. was responsible for analyzing the stomatal and vein photos. H.B. was responsible for analyzing the data and writing the manuscript. S.P. was the principal investigator and laboratory leader, and responsible for reviewing final manuscript. F.W. was responsible for the experimental design, analyzing the data, writing the manuscript, and drawing the figures with L.W.

REFERENCES

Beerling, D. J., & Franks, P. J. (2010). Plant science: The hidden cost of transpiration. *Nature*, *464*, 495–496. https://doi.org/10.1038/464495a

Boyce, C. K., Brodribb, T. J., Field, T. S., & Zwieniecki, M. A. (2009). Angiosperm leaf vein evolution was physiologically and environmentally transformative. *Proceedings of the Royal Society B: Biological Sciences*, *276*, 1771–1776. https://doi.org/10.1098/rspb.2008.1919

Brodribb, T. J., & Jordan, G. J. (2007). Leaf maximum photosynthetic rate and venation are linked by hydraulics. *Plant Physiology*, *144*, 1890–1898. https://doi.org/10.1104/pp.107.101352

Brodribb, T. J., & Jordan, G. J. (2011). Water supply and demand remain balanced during leaf acclimation of *Nothofagus cunninghamii* trees. *The New phytologist*, *192*, 437–448. https://doi.org/10.1111/j.1469-8137.2011.03795.x

Brodribb, T. J., Jordan, G. J., & Carpenter, R. J. (2013). Unified changes in cell size permit coordinated leaf evolution. *The New Phytologist*, *199*, 559–570. https://doi.org/10.1111/nph.12300

Brodribb, T. J., McAdam, S. A., & Carins Murphy, M. R. (2017). Xylem and stomata, coordinated through time and space. *Plant, Cell and Environment*, *40*, 872–880. https://doi.org/10.1111/pce.12817

Campbell, G. S., & Norman, J. M. 1998. *Introduction to environmental biophysics* (2nd ed). New York, NY: Springer.

Cardoso, A., Randall, J. M., Jordan, G. J., & McAdam, S. A. M. (2018). Extended differentiation of veins and stomata is essential for the expansion of large leaves in *Rheum rhabarbarum*. *American Journal of Botany*, *105*, 1967–1974. https://doi.org/10.1002/ajb2.1196

Caringella, M. A., Bongers, F. J., & Sack, L. (2015). Leaf hydraulic conductance varies with vein anatomy across *Arabidopsis thaliana* wild-type and leaf vein mutants. *Plant, Cell and Environment*, *38*, 2735–2746. https://doi.org/10.1111/pce.12584

Cassman, K. G. (1999). Ecological intensification of cereal production systems: Yield potential, soil quality, and precision agriculture. *Proceedings of the National Academy of Sciences*, *96*, 5952–5959. https://doi.org/10.1073/pnas.96.11.5952

Challinor, A. J., Watson, J., Lobell, D. B., Howden, S. M., Smith, D. R., & Chhetri, N. (2014). A meta-analysis of crop yield under climate change and adaptation. *Nature Climate Change*, *4*, 287–291. https://doi.org/10.1038/nclimate2153

Coomes, D. A., Heathcote, S., Godfrey, E. R., Shepherd, J. J., & Sack, L. (2008). Scaling of xylem vessels and veins within the leaves of oak species. *Biology Letters*, *4*, 302–306. https://doi.org/10.1098/rsbl.2008.0094

Crafts-Brandner, S. J., & Salvucci, M. E. (2000). Rubisco activase constrains the photosynthetic potential of leaves at high temperature and CO_2. *Proceedings of the National Academy of Sciences*, *97*, 13430–13435. https://doi.org/10.1073/pnas.230451497

de Boer, H. J., Price, C. A., Cremer, W. F., Dekker, S. C., Franks, P. J., & Veneklaas, E. J. (2016). Optimal allocation of leaf epidermal area for gas exchange. *The New Phytologist*, *210*, 1219–1228. https://doi.org/10.1111/nph.13929

de Boer, H. J., Eppinga, M. B., Wassen, M. J., & Dekker, S. C. (2012). A critical transition in leaf evolution facilitated the cretaceous angiosperm revolution. *Nature Communications*, *3*, 1221. https://doi.org/10.1038/ncomms2217

Defraeye, T., Verboven, P., Ho, Q. T., & Nicolai, B. (2013). Convective heat and mass exchange predictions at leaf surfaces: Applications, methods and perspectives. *Computers and Electronics in Agriculture*, *96*, 180–201. https://doi.org/10.1016/j.compag.2013.05.008

Drake, P. L., Froend, R. H., & Franks, P. J. (2013). Smaller, faster stomata: Scaling of stomatal size, rate of response, and stomatal conductance. *Journal of Experimental Botany*, *64*, 495–505. https://doi.org/10.1093/jxb/ers347

Endo, M., Tsuchiya, T., Hamada, K., Kawamura, S., Yano, K., Ohshima, M., … Kawagishi-Kobayashi, M. (2009). High temperatures cause male sterility in rice plants with transcriptional alterations during pollen development. *Plant & Cell Physiology*, *50*, 1911–1922. https://doi.org/10.1093/pcp/pcp135

Farquhar, G. D., & Sharkey, T. D. (1982). Stomatal conductance and photosynthesis. *Annual Review of Plant Physiology and Plant Molecular Biology*, *33*, 317–345. https://doi.org/10.1146/annurev.pp.33.060182.001533

Farquhar, G. D., Ehleringer, J. R., & Hubick, K. T. (1989). Carbon isotope discrimination and photosynthesis. *Annual Review of Plant Physiology and Plant Molecular Biology*, *40*, 503–537. https://doi.org/10.1146/annurev.pp.40.060189.002443

Franks, P. J., & Beerling, D. J. (2009). Maximum leaf conductance driven by CO_2 effects on stomatal size and density over geologic time. *Proceedings of the National Academy of Sciences*, *106*, 10343–10347. https://doi.org/10.1073/pnas.0904209106

Franks, P. J., & Beerling, D. J. (2010). CO_2-forced evolution of plant gas exchange capacity and water-use efficiency over the phanerozoic. *Geobiology*, *7*, 227–236. https://doi.org/10.1111/j.1472-4669.2009.00193.x

Franks, P. J., Royer, D. L., Beerling, D. J., Water, P. K. V.D., Cantrill, D. J., Barbour, M. M., & Berry, J. A. (2014). New constraints on atmospheric CO_2 concentration for the phanerozoic. *Geophysical Research Letters*, *41*, 4685–4694. https://doi.org/10.1002/2014GL060457

Franks, P. J., Leitch, I. J., Elizabeth, M. R., Hetherington, A. M., & Beerling, D. J. (2012). Physiological framework for adaptation of stomata to CO_2 from glacial to future concentrations. *Philosophical transactions of the Royal Society of London. Series B: Biological Sciences*, *367*, 537–546. https://doi.org/10.1098/rstb.2011.0270

Gandin, A., Koteyeva, N. K., Voznesenskaya, E. V., Edwards, G. E., & Cousins, A. B. (2014). The acclimation of photosynthesis and respiration to temperature in the C_3-C_4 intermediate *Sasola divaricate*: Induction of high respiratory CO_2 release under low temperature. *Plant, Cell and Environment*, *37*, 2601–2612. https://doi.org/10.1111/pce.12345

Gourdji, S. M., Sibley, A. M., & Lobell, D. B. (2013). Global crop exposure to critical high temperatures in the reproductive period: Historical trends and future projections. *Environmental Research Letters*, *8*, 024041. https://doi.org/10.1088/1748-9326/8/2/024041

Hetherington, A. M., & Woodward, F. I. (2003). The role of stomata in sensing and driving environmental change. *Nature*, *424*, 901–908. https://doi.org/10.1038/nature01843

Huang, G. J., Zhang, Q. Q., Wei, X. H., Peng, S., & Li, Y. (2017). Nitrogen can alleviate the inhibition of photosynthesis caused by high temperature stress under both steady-state and flecked irradiance. *Frontier of Plant Science*, *8*. https://doi.org/10.3389/fpls.2017.00945

Huang, L. Y., Yang, D. S., Li, X. X., Peng, S. B., & Wang, F. (2019). Coordination of high grain yield and high nitrogen use efficiency through large sink size and high post-heading source capacity in rice. *Field Crops Research*, *233*, 49–58. https://doi.org/10.1016/j.fcr.2019.01.005

Hubbard, R. M., Ryan, M. G., Stiller, V., & Sperry, J. S. (2001). Stomatal conductance and photosynthesis vary linearly with plant hydraulic conductance in Ponderosa pine. *Plant, Cell and Environment*, *24*, 113–121. https://doi.org/10.1046/j.1365-3040.2001.00660.x

Kaiser, E., Morales, A., Harbinson, J., Heuvelink, E., Prinzenberg, A. E., & Marcelis, L. F. M. (2016). Metabolic and diffusional limitations of photosynthesis in fluctuating irradiance in *Arabidopsis thaliana*. *Science Reports*, *6*. https://doi.org/10.1038/srep31252

Khush, G. S. (2001). Green revolution: The way forward. *Nature Reviews Genetics*, *2*. https://doi.org/10.1038/35093585

Koester, R. P., Nohl, B. M., Diers, B. W., & Ainsworth, E. A. (2016). Has photosynthetic capacity increased with 80 years of soybean breeding? An examination of historical soybean cultivars. *Plant, Cell and Environment*, *39*, 1058–1067. https://doi.org/10.1111/pce.12675

Koester, R. P., Skoneczka, J. A., Cary, T. R., Diers, B. W., & Ainsworth, E. A. (2014). Historical gains in soybean (*Glycine max Merr.*) seed yield are driven by linear increases in light interception, energy conversion, and partitioning efficiencies. *Journal of Experimental Botany*, *65*, 3311–3321. https://doi.org/10.1093/jxb/eru187

Koike, S., Yamaguchi, T., Ohmori, S., Hayashi, T., Yatou, O., & Yoshida, H. (2015). Cleistogamy decreases the effect of high temperature stress at flowering in rice. *Plant Production Science*, *18*, 111–117. https://doi.org/10.1626/pps.18.111

Kusumi, K., Hirotsuka, S., Kumamaru, T., & Iba, K. (2012). Increased leaf photosynthesis caused by elevated stomatal conductance in a rice mutant deficient in SLAC1, a guard cell anion channel protein. *Journal of Experimental Botany*, *63*, 5635–5644. https://doi.org/10.1093/jxb/ers216

Lawson, T., & Vialet-Chabrand, S. (2019). Speedy stomata, photosynthesis and plant water use efficiency. *The New Phytologist*, *221*, 93–98. https://doi.org/10.1111/nph.15330

Liu, C., Ou, S., Mao, B., Tang, J., Wang, W., Wang, H., … Chu, C. (2018). Early selection of *bZIP73* facilitated adaptation of *japonica* rice to cold climates. *Nature Communications*, *9*, 3302. https://doi.org/10.1038/s41467-018-05753-w

Long, S. P., Marshallcolon, A., & Zhu, X. G. (2015). Meeting the global food demand of the future by engineering crop photosynthesis and yield potential. *Cell*, *161*, 56–66. https://doi.org/10.1016/j.cell.2015.03.019

Lu, Z., Percy, R. G., Qualset, C. O., & Zeiger, E. (1998). Stomatal conductance predicts yields in irrigated pima cotton and bread wheat grown at high temperatures. *Journal of Experimental Botany*, *49*, 453–460. https://doi.org/10.1093/jxb/49.Special_Issue.453

Ma, Y., Dai, X., Xu, Y., Luo, W., Zheng, X., Zeng, D., … Chong, K. (2015). *COLD1* confers chilling tolerance in rice. *Cell*, *160*, 1209–1221. https://doi.org/10.1016/j.cell.2015.01.046

McAdam, S. A. M., Eleouet, M. P., Best, M., Brodribb, T. J., Murphy, M. C., Cook, S. D., … Urquhart, S. (2017). Linking auxin with photosynthetic rate via leaf venation. *Plant Physiology*, *175*, 351–360. https://doi.org/10.1104/pp.17.00535

McAusland, L., Vialet-Chabrand, S., Davey, P., Baker, N. R., Brendel, O., & Lawson, T. (2016). Effects of kinetics of light-induced stomatal responses on photosynthesis and water-use efficiency. *The New Phytologist*, *211*, 1209–1220. https://doi.org/10.1111/nph.14000

McElwain, J. C., Yiotis, C., & Lawson, T. (2016). Using modern plant trait relationships between observed and theoretical maximum stomatal conductance and vein density to examine patterns of plant macroevolution. *The New Phytologist*, *209*, 94–103. https://doi.org/10.1111/nph.13579

Radoglou, K. M., & Jarvis, P. G. (1990). Effects of CO_2 enrichment on four poplar clones. ii. Leaf surface properties. *Annals of Botany*, *65*, 627–632. https://doi.org/10.1093/oxfordjournals.aob.a087979

Ramankutty, N., Mehrabi, Z., Waha, K., Jarvis, L., Kremen, C., Herrero, M., & Rieseberg, L. (2018). Trends in global agricultural land use: Implications for environmental health and food security. *Annual Review of Plant Biology*, *69*, 789–815. https://doi.org/10.1146/annurev-arplant-042817-040256

Roche, D. (2015). Stomatal conductance is essential for higher yield potential of C_3 crops. *Critical Reviews in Plant Sciences*, *34*, 429–453. https://doi.org/10.1080/07352689.2015.1023677

Sack, L., & Scoffoni, C. (2013). Leaf venation: Structure, function, development, evolution, ecology and applications in the past, present and future. *The New Phytologist*, *198*, 983–1000. https://doi.org/10.1111/nph.12253

Sage, R. F., & Kubien, D. S. (2007). The temperature response of C_3 and C_4 photosynthesis. *Plant, Cell and Environment*, *30*, 1086–1106. https://doi.org/10.1007/s11120-013-9874-6.

Shah, F., Nie, L., Cui, K., Shah, T., Wu, W., Chen, C., … Huang, J. (2014). Rice grain yield and component responses to near 2 °C of warming. *Field Crops Research*. *157*, 98–110. https://doi.org/10.1016/j.fcr.2013.12.014

Takahashi, S., & Murata, N. (2008). How do environmental stresses accelerate photoinhibiton? *Trends in Plant Science*, *13*, 178–182. https://doi.org/10.1016/j.tplants.2008.01.005

Tanaka, Y., Sugano, S. S., Shimada, T., & Hara-Nishimura, I. (2013). Enhancement of leaf photosynthetic capacity through increased stomatal density in *Arabidopsis*. *The New Phytologist*, *198*, 757–764. https://doi.org/10.1111/nph.12186

Taneda, H., & Terashima, I. (2012). Coordinated development of the leaf midrib xylem with the lamina in *Nicotiana tabacum*. *Annals of Botany*, *110*, 35–45. https://doi.org/10.1093/aob/mcs102

Taylaran, R. D., Adachi, S., Ookawa, T., Usuda, H., & Hirasawa, T. (2011). Hydraulic conductance as well as nitrogen accumulation plays a role in the higher rate of leaf photosynthesis of the most productive variety of rice in Japan. *Journal of Experimental Botany*, *62*, 4067–4077. https://doi.org/10.1093/jxb/err126

Tholen, D., Boom, C., & Zhu, X. G. (2012). Opinion: Prospects for improving photosynthesis by altering leaf anatomy. *Plant Science*, *197*, 92–101. https://doi.org/10.1016/j.plantsci.2012.09.005

Wong, S. C., Cowan, I. R., & Farquhar, G. D. (1979). Stomatal conductance correlates with photosynthetic capacity. *Nature*, *282*, 424–426. https://doi.org/10.1038/282424a0

Xiong, D., Ling, X., Huang, J., & Peng, S. (2017). Meta-analysis and dose-response analysis of high temperature effects on rice yield and quality. *Environmental and Experimental Botany*, *141*, 1–9. https://doi.org/10.1016/j.envexpbot.2017.06.007

Xiong, D. L., Yu, T. T., Zhang, T., Li, Y., Peng, S. B., & Huang, J. L. (2015). Leaf hydraulic conductance is coordinated with leaf morpho-anatomical traits and nitrogen status in the genus *Oryza*. *Journal of Experimental Botany*, *66*, 741–748. https://doi.org/10.1093/jxb/eru434

Yamori, W., Hikosaka, K., & Way, D. A. (2014). Temperature response of photosynthesis in C_3, C_4, and CAM plants: Temperature acclimation and temperature adaptation. *Photosynthesis Research*, *119*, 101–117. https://doi.org/10.1007/s11120-013-9874-6

Yuan, L. (1997). Hybrid rice breeding for super high yield. *Hybrid Rice*, *12*, 1–6.

Zhang, F. P., Murphy, M. R. C., Cardoso, A. A., Jordan, G. J., & Brodribb, T. J. (2018). Similar geometric rules govern the distribution of veins and stomata in petals, sepals and leaves. *The New Phytologist*, *219*, 1224–1234. https://doi.org/10.1111/nph.15210

Zhao, C., Piao, S., Wang, X., Huang, Y., Ciais, P., Elliott, J., … Peñuelas, J. (2016). Plausible rice yield losses under future climate warming. *Nature Plants*, *3*. https://doi.org/10.1038/nplants.2016.202

Zhu, G., Peng, S., Huang, J., Cui, K., Nie, L., & Wang, F. (2016). Genetic improvements in rice yield and concomitant increases in radiation- and nitrogen-use efficiency in middle reaches of Yangtze River. *Scientific Reports*, *6*. https://doi.org/10.1038/srep21049

SUPPORTING INFORMATION

Additional supporting information may be found online in the Supporting Information section at the end of the article.

How to cite this article: Wu L, de Boer HJ, Zixiao Z, et al. The coordinated increase in stomatal density and vein dimensions during genetic improvement in rice. *Agronomy Journal*. 2020;112:2791–2804. https://doi.org/10.1002/agj2.20180